BB

PREPRINT

tascc

TASCC-P-96-13

SECONDARY DECAY AND TWO-FRAGMENT CORRELATION FUNCTIONS

D. Fox[a] *, D.R. Bowman[a], G.C. Ball[a], L. Beaulieu[b], B. Djerroud[b] †, D. Doré[b] ‡, W.A. Friedman[c], A. Galindo-Uribarri[a], E. Hagberg[a], D. Horn[a], R. Laforest[b] §, Y. Larochelle[b], R. Roy[b] and C. St-Pierre[b]

[a] *AECL, Chalk River Laboratories, Chalk River, Ontario K0J 1J0, Canada*
[b] *Laboratoire de Physique Nucléaire, Département de Physique, Université Laval, Ste-Foy, Québec G1K 7P4, Canada*
[c] *Department of Physics, University of Wisconsin, Madison, Wisconsin 53706, USA*

CERN LIBRARIES, GENEVA
SCAN-9606013

* Present Address: Practical Political Consulting, East Lansing, MI 48823, USA
† Present Address: NSRL, University of Rochester, Rochester, NY 14627, USA
‡ Present Address: Institut de Physique Nucléaire d'Orsay, B.P. 91406 Orsay Cedex, France
§ Present Address: Chalk River Laboratories, Chalk River, Ontario K0J 1J0, Canada

Submitted to
Phys. Rev. C (Rapid Comm.)

Sw9624

NOTICE

This report is not a formal publication; if it is cited as a reference, the citation should indicate that the report is unpublished. To request copies our E-mail address is **TASCC@CRL.AECL.CA.**

Physical and Environmental Sciences
Chalk River Laboratories
Chalk River, ON K0J 1J0 Canada

1996 April

Secondary Decay and Two-Fragment Correlation Functions

D. Fox[a*], D.R. Bowman[a], G.C. Ball[a], L. Beaulieu[b], B. Djerroud[b†], D. Doré[b‡], W.A. Friedman[c], A. Galindo-Uribarri[a], E. Hagberg[a], D. Horn[a], R. Laforest[b§], Y. Larochelle[b], R. Roy[b], and C. St-Pierre[b]

[a] *AECL, Chalk River Laboratories, Chalk River, Ontario K0J 1J0, Canada*

[b] *Laboratoire de Physique Nucléaire, Département de Physique, Université Laval, Ste-Foy, Québec G1K 7P4, Canada*

[c] *Department of Physics, University of Wisconsin, Madison, Wisconsin 53706, USA*

Abstract

Two-fragment reduced-velocity and azimuthal-angle correlations have been measured in ^{70}Ge + ^{27}Al reactions at E/A = 22 and 35 MeV. The mixed-fragment ($3 \leq Z \leq 9$) emission time scales extracted from comparisons with schematic three-body trajectory simulations are in qualitative agreement with predictions of a sequential evaporation model. However, the inferred emission time scales decrease strongly with increasing fragment charge, in disagreement with predictions by the model and with published results based upon pre- and post-scission neutron multiplicites. The decay of an emitted primary fragment into two observed secondary fragments is investigated as a possible cause for the apparent charge-dependence of the fragment emission time scale.

---

*Present address: Practical Political Consulting, East Lansing MI 48823, USA

†Present address: NSRL, University of Rochester, Rochester N.Y. 14627, USA

‡Present address: Institut de Physique Nucléaire d'Orsay, B.P. 91406 Orsay Cedex, France

§Present address: Chalk River Laboratories, Chalk River, Ontario K0J 1J0, Canada

Correlations between emitted nuclear fragments provide information about the lifetime [1–8] and collective behavior [6,9] of excited nuclear matter. While much experimental work has demonstrated that the time scale for multiple fragment emission becomes very short at bombarding energies of $E/A \geq 50$ MeV [2,4,5], there has been no determination of the time scale for fragment emission near the threshold for the process. Although multiple emission near threshold may represent only a small fraction of the total reaction cross section, such a study would investigate most sensitively whether the fragment emission time scale evolves in a manner predicted by sequential, statistical decay mechanisms [10,11].

Additional properties of the decaying systems may be obtained from the dependence of two-fragment correlation functions on observables such as the fragment energy [7] or the orientation of the fragment-fragment relative velocity vector [3]. Studies of pre- and post-scission neutron multiplicities have indicated a strong mass dependence of the fragment emission time scale, presumably associated with a pre- or post-saddle dynamical hindrance [12–14]. Two-fragment correlation functions gated on fragment charge may allow the mass dependence of the emission time scale to be quantified and provide an additional probe into the dynamics of nuclear collective motion.

To study multiple fragment emission near the threshold for the process, a series of experiments was performed at the Tandem Accelerator Superconducting Cyclotron (TASCC) Facility at the Chalk River Laboratories. Beams of ^{70}Ge with energies of $E/A = 22$ and 35 MeV and intensities of 0.2 and 0.1 nA, respectively, impinged upon ^{27}Al targets with thicknesses of 1 mg/cm^2 ($E/A = 22$ MeV) and 2 mg/cm^2 ($E/A = 35$ MeV). Fragments with $Z < 20$ were detected and identified with a 48-element phoswich array [15] located at $\theta_{lab} = 6.9° - 24°$. Typical detector thresholds were E/A = 8.5, 14.5, and 17.5 MeV for fragments of $Z = 2$, 6, and 9, respectively. Energy calibrations were performed with the procedure of Ref. [16], and are estimated to be accurate to approximately 10%. Additional fragments and particles were detected in a 32-element CsI(Tl) array [17] located at $\theta_{lab} = 24°$

to 45°. In the $E/A = 22$ MeV reaction, 24 thin CsI(Tl) detectors [18] covered approximately 70% of the solid angle between $\theta_{lab} = 45°$ and 154°. The CsI(Tl) detectors at $\theta_{lab} \geq 24°$ provided additional multiplicity information for particles and fragments with $E/A > 2$ MeV.

The two-fragment reduced-velocity correlation function $R(v_{red})$ is defined as the ratio of the coincidence to the singles yields:

$$1 + R(v_{red}) = C \sum_{\mathbf{v_1},\mathbf{v_2}} \frac{Y_{12}(\mathbf{v_1},\mathbf{v_2})}{Y_1(\mathbf{v_1})Y_2(\mathbf{v_2})}, \qquad (1)$$

where $\mathbf{v_1}$ and $\mathbf{v_2}$ are the laboratory velocities of the two fragments, v_{red} is the reduced relative velocity, $v_{red} = (\mathbf{v_1} - \mathbf{v_2})/\sqrt{Z_1 + Z_2}$, and C is a normalization constant equal to $\sum_{\mathbf{v_1},\mathbf{v_2}} \sum_{v_{red}} Y_1(\mathbf{v_1})Y_2(\mathbf{v_2})/Y_{12}(\mathbf{v_1},\mathbf{v_2})$. The background yield, $Y_1(\mathbf{v_1})Y_2(\mathbf{v_2})$, is constructed by selecting fragments from different events.

Correlation functions gated by atomic number are shown in Fig. 1 ($E/A = 22$ MeV) and Fig. 2 ($E/A = 35$ MeV) for fragments detected between $\theta_{lab} = 6.9°$ and 24°. Gating on charged-particle multiplicity does not affect the experimental correlation functions significantly, which suggests that in these reactions the emission of two fragments may be a better event selector than the charged-particle multiplicity.

In order to quantify the fragment emission time scales, the data were compared with predictions of three-body trajectory simulations [3]. Calculations assuming a source charge $Z_S = 25$, a source radius $R_S = 8$ fm, and a source velocity, v_S, intermedate between the beam velocity and the center of mass velocity, are shown in Figs. 1 and 2 (curves) for different mean fragment emission times. The mean emission time inferred for fragments with $3 \leq Z_1, Z_2 \leq 9$ decreases from ≈ 500 fm/c in the $E/A = 22$ MeV reaction (Fig. 1(a)) to ≈ 200 fm/c for the $E/A = 35$ MeV reaction (Fig. 2(a)).

These extracted time scales can be compared with predictions from a sequential decay model [8]. Nucleon transport model calculations (BNV) [19] were performed to provide input for the Expanding Emitting Source (EES) model [11]. The predicted fragment emission time scales of 300-400 fm/c for the $E/A = 22$ MeV reaction and 200-300 fm /c for the $E/A = 35$ MeV reaction are in reasonable agreement with the time scales extracted from the three-body trajectory calculations.

While the three-body calculations fail to reproduce the enhancement in the correlation functions at $v_{red} = 0.02c$, they do reproduce the observed rise for heavy fragment pairs at $v_{red} > 0.03c$ (panels (c) and (d)). This rise is a consequence of the (high) recoil velocity of the $Z_S = 25$ source following emission of the first fragment; calculations assuming a more massive source of $Z_S = 45$ (open circles) do not reproduce the rise. Because the heavy fragment correlation functions are most sensitive to the source recoil velocity, the rise at $v_{red} > 0.03c$ suggests only that *the source charge for the heavier fragments is* $Z_S \approx 25$. Lighter fragments and particles could be emitted from more massive sources. This mechanism would be consistent with a decay chain in which the light particles and the light fragments are emitted earlier, on average, that the heavy fragments [12–14].

In contrast, the rising portion of the correlation functions ($v_{red} < 0.02$ c) imply that the fragment emission time scale decreases strongly with increasing charge. The inferred decrease from 1000 fm/c or more for $3 \leq Z_1, Z_2 \leq 4$ (panels (b)) to 100-200 fm/c for $7 \leq Z_1, Z_2 \leq 9$ (panels (d)) is insensitive to changes in the parameters of the trajectory calculations. Previous experimental work has also suggested a slight decrease in the emission time scale with increasing fragment charge [1]. However, these results are in contradiction with studies of pre- and post-scission neutron multiplicities which indicate an increase in emission time with increasing charge [12–14], and with the EES calculations which predict no significant change in the characteristic emission time with charge. In order to explain this inconsistency, we have investigated other effects which can influence the time scales extracted from two-fragment correlation functions.

Nuclear collective motion strongly affects two-fragment correlation functions, particularly in non-central collisions where the angular momentum is largest [6]. To investigate the magnitude of nuclear rotation, azimuthal-angle correlation functions (not shown) were constructed for like-fragment pairs detected between 6.9° and 24°. The effect of rotation was schematically incorporated into the three-body trajectory calculations by weighting the relative azimuthal emission angle between the two emitted fragments as

$P(\Delta\phi) \propto 1+\lambda_2 \cos(2\Delta\phi)$ [9]. Calculations with $\lambda_2 \neq 0$ provide improved agreement with the azimuthal angle correlation functions over those with no in-plane focussing. However, the trajectory calculations cannot fit the azimuthal angle correlation function at *both* $\Delta\phi = 0°$ and 180° without including effects of both rotation *and* directed transverse motion (flow) which enhances the azimuthal correlation at $\Delta\phi = 0°$ [9].

For asymmetric reactions at bombarding energies of 22A and 35A MeV, the directed transverse motion should be small. Recently, the influence of secondary decay on light-particle correlation functions has been demonstrated [20,21]. Secondary decay into fragment pairs should also affect two-fragment correlation functions.

To investigate the magnitude of this process, we have performed calculations with the sequential-decay code GEMINI [10] using input parameters predicted by the BNV model. The correlation function predicted by GEMINI for the E/A = 22 MeV reaction is shown as the solid curve in Fig. 3(a). Fragment pairs were found to be produced by two mechanisms: 1) primary pairs emitted sequentially from the cooling compound nucleus (dashed curve), and 2) secondary pairs produced by the division of a primary parent ("mitotic" pairs, dotted curve).

The correlation function for the mitotic pairs shows a strongly peaked distribution centered at a value of v_{red} corresponding to the average Coulomb barrier between the two fragments. The correlation function for the other (non-mitotic) fragments is similiar to the correlation functions predicted by the three-body trajectory calculation for very long emission time scales. In order to introduce realistic fragment emission time scales into GEMINI, the charge, energy, and angular distributions predicted for the non-mitotic pairs were sampled with the three-body trajectory calculation, and two-fragment correlation functions were generated with mean emission times of 0, 200, 500, 1000, and 5000 fm/c (Fig. 3(b)). As with the calculations shown in Figs. 1 and 2 which used the experimental distributions, best agreement is obtained for a mean emission time of 500 fm/c, although, as above, the bump in the correlation function near $v_{red} = 0.02c$ is not reproduced.

Comparison of the data with the complete GEMINI calculation in Fig. 3(a) (solid curve) indicates that the calculation greatly overpredicts (40%) the amount of secondary decay (mitotic pairs) which contributes to the two-fragment correlation functions. However, smaller admixtures of secondary decay allow improved agreement with the data. In Fig. 3(c) calculations for E/A = 22 MeV with τ = 200 and 500 fm/c are shown (from Fig. 3(b)), along with a τ = 200 calculation which includes an 18% admixture of pairs produced by the mitosis mechanism (solid curve). The agreement of the latter calculation with data is much improved over that of any of the three-body trajectory calculations. Improved agreement with the data can be obtained for the E/A = 35 MeV reaction with an emission time scale of $\tau = 0$ fm/c and a 9% admixture of mitotic pairs (Fig. 3(d)). Similarly good agreement with the azimuthal-angle correlation functions may be obtained by allowing an atomic number dependence of the mitosis fraction.

Good fits to the experimental correlation functions can be obtained for a range of emission time scales and mitosis fractions, thus making time scale determinations difficult. However, combinatoric arguments suggest that the mitosis fraction should be larger at lower energy where the fragment multiplicity is lower [1].

GEMINI predicts an approximate charge-independence of v_{red} for mitotic decay ($\approx$ 0.015 c) in contrast to the observed shift of the rising part of the correlation function to smaller v_{red} with decreasing fragment charge. Mitotic decay may also occur for smaller values of v_{red} via a barrier penetration process which is not considered by GEMINI. The Coulomb transmission probabilities for several symmetric decays have been calculated with the WKB approximation [22]. For decays with $l = 0$ the transmission probability at $v_{red} \approx 0.012$ is approximately 0.1 for symmetric ^{12}C decay as compared to approximately 0.01 for symmetric decay of ^{24}Mg and ^{36}Ar fragments; with $l > 0$ the transmission probability at $v_{red} \approx 0.012$

[1]For a fixed fraction of secondary decay, f, and a fragment multiplicity N_{IMF}, the fraction of secondary pairs contributing to the correlation function will be $f/(N_{IMF}-1)$

is ≈ 0.05 for ^{12}C decay as compared to 0.01 for ^{24}Mg and ^{36}Ar decay[2]. The increased probability for sub-barrier mitotic decay may explain the observed shift of the rising portion of the correlation function to smaller v_{red} with decreasing fragment charge.

Along with modification of the inferred emission time scales, secondary decays also mimic the effect of directed transverse motion and may introduce uncertainties into the extraction of flow parameters [9]. It should be noted that an extraction of flow from the in-plane transverse momentum [23], which is a global event variable, is less sensitive to contamination from secondary decays than an extraction from two-particle correlations functions.

In conclusion, we have analyzed two-fragment correlation functions in $E/A = 35$ and 22 MeV ^{70}Ge + ^{27}Al reactions. Comparison of the data with schematic three-body trajectory calculations indicate mixed-fragment emission time scales of 500 and 200 fm/c for the lower and higher energy reactions, respectively, in qualitative agreement with predictions of a sequential decay model. The comparisons also suggest a charge-dependence of the emission time scale which is not predicted by the model nor consistent with the charge-dependence of fragment emission times extracted from pre- and post-scission neutron multiplicities. Secondary decays of emitted primary fragments affect the shape of correlation functions at $v_{red} < 0.02$ c, and provide a possible explanation for the anomalous dependence of the inferred emission time scale on fragment charge.

We thank the TASCC Operations Group for providing the $E/A = 35$ MeV ^{70}Ge beam which was outside the designed operating range of the cyclotron. This work was supported in part by the Natural Sciences and Engineering Research Council of Canada.

---

[2]For the decays with $l > 0$, the orbital angular momentum was assumed to be proportional to mass ($l = 1$, 2, and 3), in accordance with a thermal partition.

REFERENCES

[1] Y.D. Kim *et al.*, Phys. Rev. Lett. **67**, 14 (1991).

[2] E. Bauge *et al.*, Phys. Rev. Lett. **70**, 3705 (1993).

[3] T. Glasmacher *et al.*, Phys. Rev. C **50**, 952 (1994)

[4] D. Fox *et al.*, Phys. Rev. C **50**, 2424 (1994).

[5] M. Louvel *et al.*, Phys. Lett. B **320**, 221 (1994).

[6] R. Kotte *et al.*, Phys. Rev. C **51**, 2686 (1995).

[7] E. Cornell *et al.*, Phys. Rev. Lett. **75**, 1475 (1995).

[8] D.R. Bowman *et al.*, Phys. Rev. C **52**, 818 (1995).

[9] R.A. Lacey *et al.*, Phys. Rev. Lett. **70**, 1224 (1993).

[10] R.J. Charity *et al.*, Nucl. Phys. **A483**, 371 (1988).

[11] W.A. Friedman, Phys. Rev. Lett. **60**, 2125 (1988).

[12] D. Hilscher *et al.*, Phys. Rev. Lett. **62**, 1099 (1989).

[13] D.J. Hinde *et al.*, Phys. Rev. C **45**, 1229 (1992).

[14] M. Gui *et al.*, Phys. Rev. C **48**, 1791 (1993).

[15] C. Pruneau, *et al.*, Nucl. Instr. and Meth. **A297**, 404 (1990).

[16] D. Fox *et al.*, TASCC-P-95-24, Nucl. Instr. and Meth. in press.

[17] M. Gourde, M.Sc. Thesis, Université Laval (1993) unpublishd; M. Gourde *et al.*, to be publised.

[18] A. Galindo-Uribarri, Prog. Part. Nucl. Phys. **28**, 463 (1992).

[19] A. Bonasera *et al.*, Phys. Lett. B **221**, 233 (1989).

[20] D.O. Handzy *et al.*, Phys. Rev. Lett. **75**, 2916 (1995).

[21] R.J. Charity *et al.*, Phys Rev. C **52**, 3126, (1995).

[22] P. Morrison, in: Experimental Nuclear Physics, ed. E. Segrè (John Wiley and Sons, New York, 1953).

[23] G.D. Westfall *et al.*, Phys. Rev. Lett. **71**,1986 (1993).

FIGURES

FIG. 1. Reduced-velocity two-fragment correlation functions in E/A = 22 MeV ^{70}Ge + ^{27}Al reactions (solid points) for fragment pairs with (a) $3 \leq Z_1, Z_2 \leq 9$, (b) $3 \leq Z_1, Z_2 \leq 4$, (c) $5 \leq Z_1, Z_2 \leq 6$, and (d) $7 \leq Z_1, Z_2 \leq 9$. The curves correspond to three-body trajectory calculations for τ =100, 200, 500, and 1000 fm/c, assuming $Z_S = 25$, $R_S = 8$ fm, and $v_S = 0.18c$. The open points in panel (d) correspond to a three-body trajectory calculation with τ =200 fm/c, $Z_S = 45$, $R_S = 8$ fm, and $v_S = 0.16c$. See text for details.

FIG. 2. Reduced-velocity two-fragment correlation functions in E/A = 35 MeV ^{70}Ge + ^{27}Al reactions (solid points) for fragment pairs with (a) $3 \leq Z_1, Z_2 \leq 9$, (b) $3 \leq Z_1, Z_2 \leq 4$, (c) $5 \leq Z_1, Z_2 \leq 6$, and (d) $7 \leq Z_1, Z_2 \leq 9$. The curves correspond to three-body trajectory calculations for τ =100, 200, 500, and 1000 fm/c, assuming $Z_S = 25$, $R_S = 8$ fm, and $v_S = 0.23c$. The open points in panel (d) correspond to a three-body trajectory calculation with τ =100 fm/c, $Z_S = 45$, $R_S = 8$ fm, and $v_S = 0.20c$.

FIG. 3. (a) Two-fragment ($3 \leq Z \leq 9$) reduced-velocity correlation functions predicted by GEMINI. The solid curve corresponds to all emitted pairs, the dotted curve to "mitotic" pairs (see text), and the dashed curve to other (non-mitotic) pairs. (b) The experimental correlation function (solid points) compared with three-body trajectory calculations (curves) with the charge, energy, and angular distributions predicted by the GEMINI, and varying mean emission time scales, τ. (c) The experimental correlation function (E/A = 22 MeV) compared to three-body trajectory calculations with mean fragment emission times, τ, equal to 200 and 500 fm/c (from (b)), and a prediction with τ = 200 fm/c including an 18% admixture of mitotic events. (d) The experimental correlation function (E/A = 35 MeV) compared to three-body trajectory calculations with mean fragment emission times, τ, equal to 0 and 200 fm/c, and a prediction with τ = 0 fm/c including an 9% admixture of mitotic events.

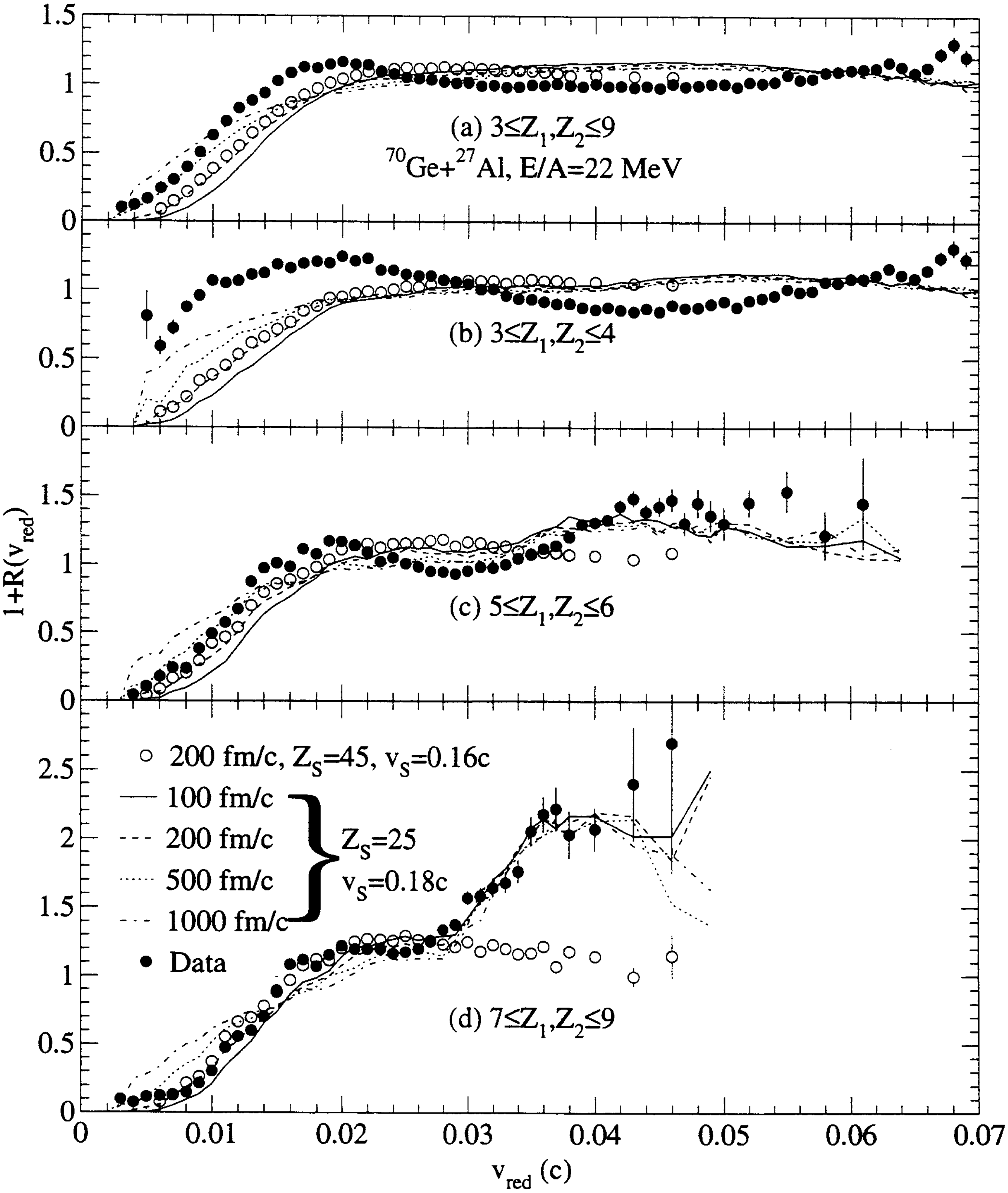

(a) 3≤Z1,Z2≤9
70Ge+27Al, E/A=22 MeV
(b) 3≤Z1,Z2≤4
(c) 5≤Z1,Z2≤6
(d) 7≤Z1,Z2≤9
200 fm/c, ZS=45, vS=0.16c
100 fm/c
200 fm/c
500 fm/c
1000 fm/c
ZS=25
vS=0.18c
Data
1+R(vred)
vred (c)

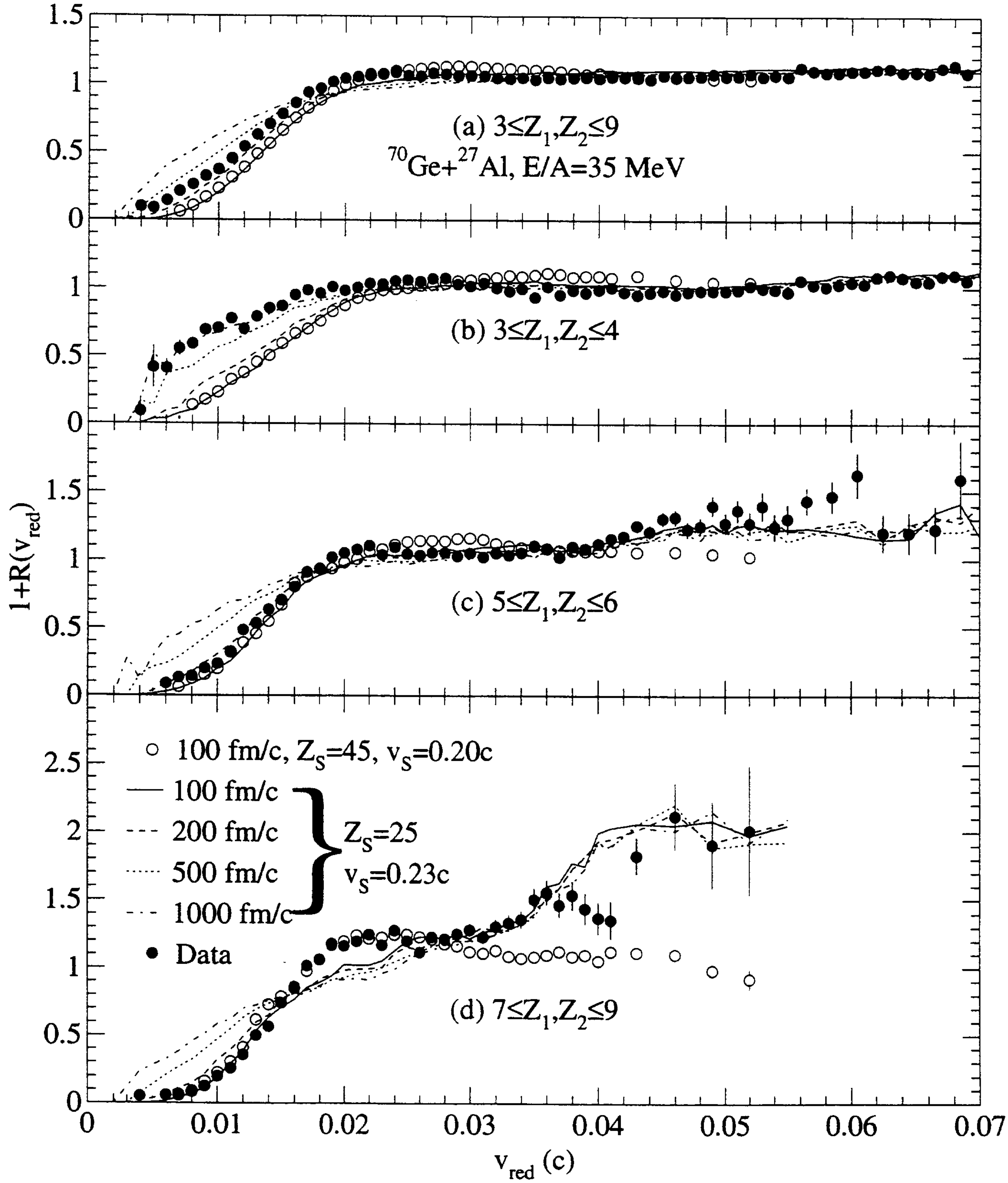
(a) 3≤Z1,Z2≤9
70Ge+27Al, E/A=35 MeV
(b) 3≤Z1,Z2≤4
(c) 5≤Z1,Z2≤6
(d) 7≤Z1,Z2≤9
100 fm/c, ZS=45, vS=0.20c
100 fm/c
200 fm/c
500 fm/c
1000 fm/c
ZS=25
vS=0.23c
Data
1+R(vred)
vred (c)
0
0.01
0.02
0.03
0.04
0.05
0.06
0.07
0.5
1
1.5
2
2.5

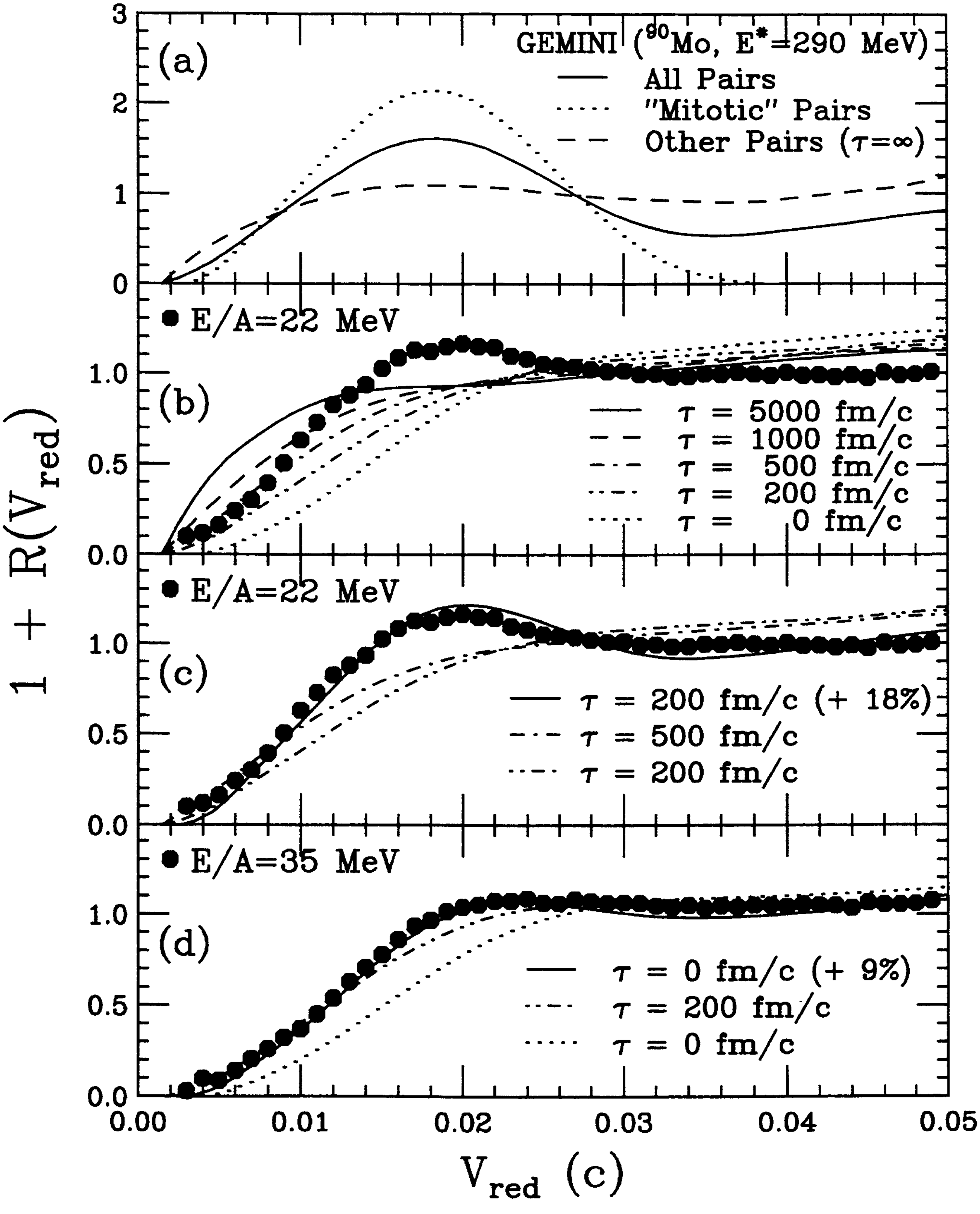

GEMINI (^{90}Mo, E*=290 MeV)
All Pairs
"Mitotic" Pairs
Other Pairs (τ=∞)
(a)
(b)
(c)
(d)
E/A=22 MeV
τ = 5000 fm/c
τ = 1000 fm/c
τ = 500 fm/c
τ = 200 fm/c
τ = 0 fm/c
E/A=22 MeV
τ = 200 fm/c (+ 18%)
τ = 500 fm/c
τ = 200 fm/c
E/A=35 MeV
τ = 0 fm/c (+ 9%)
τ = 200 fm/c
τ = 0 fm/c
1 + R(V$_{red}$)
V$_{red}$ (c)